IEEE Access
Multidisciplinary | Rapid Review | Open Access Journal

Received June 20, 2019, accepted July 8, 2019, date of publication July 23, 2019, date of current version August 9, 2019.

Digital Object Identifier 10.1109/ACCESS.2019.2930620

Compact Vertically Polarized Omnidirectional Ultra-Wideband Antenna and Its Band-Notched Filtering Application

YAOHUI ZHANG[1], YONGHONG ZHANG[1], DAOTONG LI[2,3], (Member, IEEE), ZHONGQIAN NIU[1], AND YONG FAN[1], (Member, IEEE)

[1]School of Electronic Science and Engineering, University of Electronic Science and Technology of China (UESTC), Chengdu 611731, China
[2]Center of Aerocraft TT&C and Communication, Chongqing University, Chongqing 400044, China
[3]State Key Laboratory of Millimeter Waves, Nanjing 210096, China

Corresponding author: Daotong Li (dli@cqu.edu.cn)

This work was supported in part by the National Natural Science Foundation of China under Grant 61801059, in part by the Chongqing Special Found of Technology Research and Development for Academician under Grant cstc2018zdcy-yszxX0001, and in part by the Opening subject of State Key Laboratory of Millimeter Waves under Grant K202016.

ABSTRACT This paper first proposes a 3D printed, compact, low-profile, ultra-wideband (UWB) antenna with vertically polarized omnidirectional radiation characteristics. The antenna is composed of one triangular feeding structure, one triangular shorted structure, a common capacitive top hat, and two parasitic metallic pins. Compared with traditional UWB antennas with symmetrical configuration, the proposed UWB antenna is a three-dimensional version of inverted "F" with asymmetrical structure. The proposed antenna can realize compact aperture and low profile ($0.19\lambda_L \times 0.19\lambda_L \times 0.06\lambda_L$, where λ_L is the free-space wavelength of the lowest operating frequency). Two parasitic pins are utilized to enhance the omnidirectionality of the antenna in the azimuth plane. The impedance bandwidth is greater than 10:1 (2.96–30 GHz) for VSWR < 3, and the bandwidth with horizontal radiation pattern ripple better than ± 5 dB is more than 4.9:1 (2.96–14.5 GHz). Second, this UWB design is modified to realize dual bands with a deep band-notch by adding a split gap inside the antenna. The proposed band-notched antenna is designed with the bandwidth of 2.4–2.5 and 5–10 GHz for VSWR < 2 with good horizontal radiation pattern omnidirectionality, which can be used for 2.4/5 GHz WLAN applications. The prototypes of the proposed UWB and band-notched antennas are fabricated by metallic 3D printing, and the simulated and measured results meet well.

INDEX TERMS Ultra-wideband (UWB), omnidirectional, vertically polarized, band-notch, 3D printing.

I. INTRODUCTION

Because the ultra-wideband (UWB) antennas can radiate efficiently over large frequency bands and demonstrate consistent radiation characteristics in the whole operating frequency band, they have been applied in various fields, such as the wireless communications, sensing, radar systems and microwave imaging. The physical size of an UWB antenna could be very large, since the size of the UWB antenna is primarily determined by its lowest operating frequency. Moreover, in some low-frequency applications, such as the military communications at HF, VHF and UHF bands, UWB antennas with monopole-like radiation patterns, namely the vertically polarized omnidirectional radiation patterns, are required. Low profile and small overall volume are extremely important in these applications.

Numerous types of UWB antennas with monopole-like radiation patterns have been reported in references [1]–[22]. The monopole antenna placed above a flat ground plane is the conventional way to achieve the monopole-like radiation patterns [1]–[6]. The eye-shaped monopole antenna is designed and fabricated in [1] to cover 3-20 GHz for VSWR < 1.5. The works [2]–[5] utilize conical monopole to realize vertically polarized omnidirectional patterns for ease of design and fabrication. The body-of-revolution (BoR) monopole antenna with specified radiation objectives and size constraints is designed using algorithm and optimization in [6]. Although these monopole antennas can achieve good performance, the height of the antennas are around $\lambda_L/4$ (λ_L is the free-space wavelength of the lowest operating frequency),

The associate editor coordinating the review of this manuscript and approving it for publication was Abhishek Kandwal.

which is relatively high and unsuitable for the applications with low profile.

In order to reduce the profile and volume of antenna, several techniques are employed in [7]–[19]. The capacitive ceiling-mount loading [7], [8] is adopted to lower the profile to $0.18\lambda_L$. The antennas in [9], [10] use the capacitive top hat with four shorted posts to realize low profile of around $0.07\lambda_L$. The antennas with shorted parasitic ring are fed by a crossed plate feeding structure [11] or BoR feeding structure [12]–[15] to achieve ultra-wide impedance bandwidth. The parasitic top ring with the meander line and the dielectric material is utilized in [15] to reduce the lowest frequency of operation with a diameter of $0.115\lambda_L$. The works in [16]–[19] utilizing the triangular feeding structure and a top hat with two shorted posts can realize lower profile or more compact size. The antenna in [17] can reduce the profile down to $0.033\lambda_L$, and the lateral diameter of the antenna in the azimuth plane in [19] is miniaturize to $0.14\lambda_L$. In order to compensate the radiation pattern distortion in the higher band, the work [18] realizes UWB monopole-like radiation characteristics by utilizing two antennas and an extra duplexer.

To further reduce the antenna profile and overall volume of UWB antennas, some designs [20]–[22] with extremely compact size have been reported for some specific applications. However, these designs use either resistive loading [20], [21] or lossy ferrites [22] loaded inside the antennas to achieve improved impedance matching at the cost of low realized gains.

In this paper, we firstly propose a 3D printed, compact, low-profile, UWB antenna with monopole-like radiation characteristics. Compared with the aforementioned UWB antennas with symmetrical structure, the proposed UWB antenna is a three-dimensional version of inverted "F" with asymmetrical structure. The antenna consists of one triangular feeding structure, one triangular shorted structure, a common capacitive top hat and two metallic parasitic pins. The proposed antenna can realize compact aperture and small volume ($0.19\lambda_L \times 0.19\lambda_L \times 0.06\lambda_L$). Two parasitic pins are utilized to improve the horizontal pattern ripples (± 5 dB) of the antenna. The impedance bandwidth is over 10:1 (2.96-30 GHz) for VSWR < 3, and the bandwidth with horizontal radiation pattern ripple $< \pm 5$ dB is greater than 4.9:1 (2.96-14.5 GHz). Secondly, the proposed UWB design is also modified to realize dual bands with a deep band-notch by adding a split gap inside the antenna. Without changing other parameter values, the proposed band-notched antenna can realize the bandwidth of 2.4-2.5 and 5-10 GHz for VSWR < 2 with good omnidirectional performance, which can be used for 2.4/5 GHz WLAN applications. The proposed UWB and band-notched antennas are fabricated by metallic 3D printing as demonstrations.

Four sections constitute this paper. Section II discusses the proposed UWB antenna. The band-notched antenna for WLAN applications is presented in Section III. Section IV summarizes the results obtained in this paper. The analysis is performed using 3D EM simulation software Ansys HFSS.

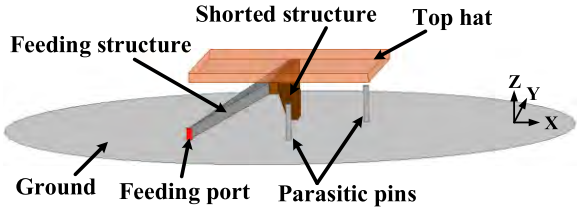

FIGURE 1. The overall structure of the proposed UWB antenna.

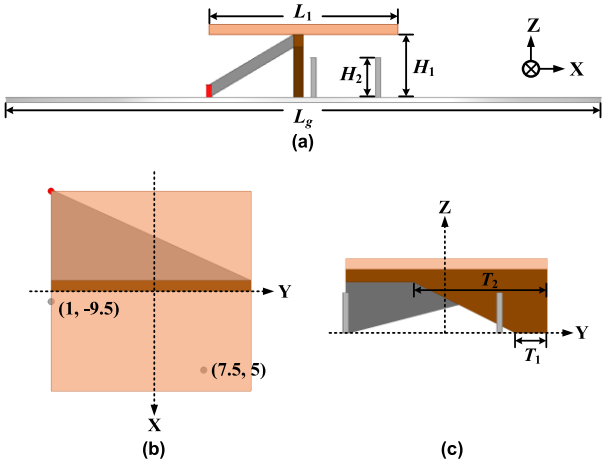

FIGURE 2. Detailed structure of the proposed UWB antenna. (a) Front side view. (b) Top view. (c) Right side view. ($L_g = 100$ mm, $L_1 = 19$ mm, $H_1 = 6$ mm, $H_2 = 3.8$ mm, $T_1 = 3$ mm, $T_2 = 13$ mm).

II. DESIGN OF UWB ANTENNA

A. STRUCTURE OF UWB ANTENNA

The overall structure of the proposed UWB antenna is shown in Fig. 1. It is composed of one triangular feeding structure, one triangular shorted structure, a common capacitive top hat and two metallic parasitic pins. The antenna is fabricated by copper 3D printing with the thickness of 1 mm. The detailed geometry of the UWB antenna is presented in Fig. 2. The square top hat with the length $L_1 = 19$ mm is placed on the middle of the circular ground. One side of the triangular feeding structure is connected in the middle of the top hat and fed by the coaxial cable below one corner of the top hat. The shorted structure is in right trapezoid shape and perpendicular with the top hat. The top hat, the feeding structure and the shorted structure intersect in one straight line. Two parasitic pins with the height of H_2 are placed at the location of (1mm, -9.5mm) and (7.5mm, 5mm) in the XOY plane inside the antenna over the metallic ground.

B. ANALYSIS OF UWB ANTENNA

In order to demonstrate the design evolution of the proposed UWB antenna, three antennas, Ant. I, Ant. II and Ant. III, are simulated and shown in Fig. 3(a), (b) and (c), respectively. Ant. I is the UWB antenna in [17] with symmetrical configuration utilizing two triangular feeding structures, two shorted structures and a square top hat. Ant. II is the proposed UWB antenna without parasitic metallic pins, and is the three-dimensional version of inverted "F"

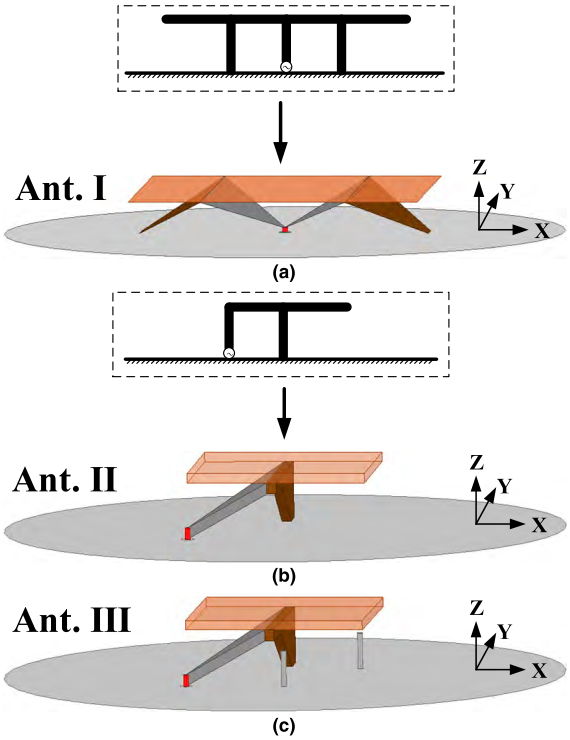

FIGURE 3. Three antennas. (a) Ant. I. (b) Ant. II. (c) Ant. III.

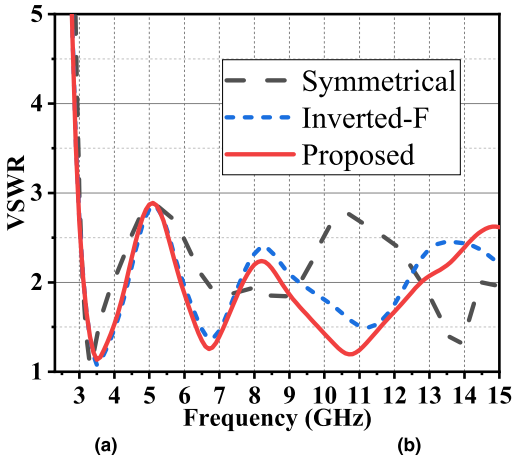

FIGURE 4. Simulated VSWRs of three antennas.

with asymmetrical structure. Ant. III is the proposed UWB antenna with two parasitic metallic pins.

These three antennas are simulated and optimized to work in the same operating frequency bands. The simulated VSWRs of three antennas are depicted in Fig. 4. The impedance bandwidths of three antennas are all more than 5:1 (3-15 GHz). The realized gains in the azimuth plane (XOY) of three antennas are displayed in Fig. 5. Although Ant. I can achieve good omnidirectional performance in the lower band, the radiation patterns at the higher frequencies are distorted due to the high resonant modes. The realized gain in the azimuth plane is smaller than −10 dBi at 8 GHz. The radiation pattern splits into two beams at 11 GHz,

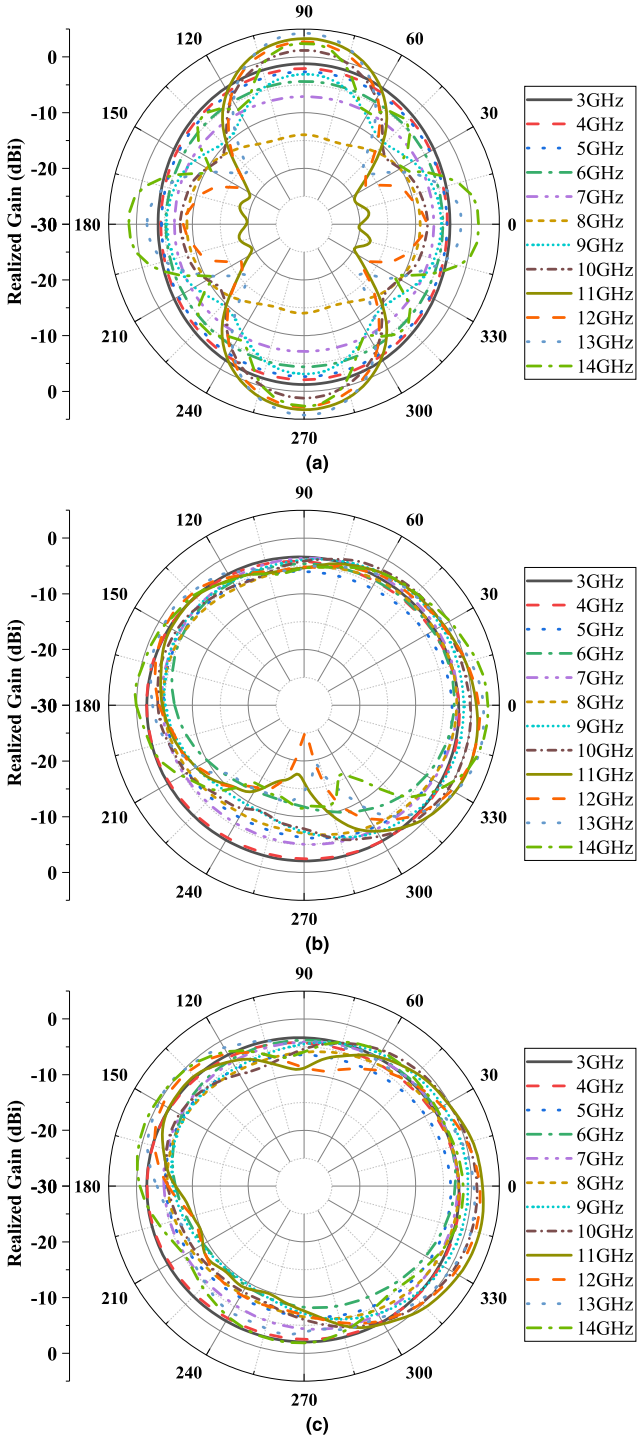

FIGURE 5. Realized gains in the azimuth plane (XOY) of three antennas. (a) Ant. I. (b) Ant. II. (c) Ant. III.

and splits into four beams at 14 GHz. Ant. II with asymmetrical structure can generate more stable realized gain in the azimuth plane. However, there are distortions at the frequencies over 11 GHz. Ant. III (proposed UWB antenna) can realize good omnidirectionality over 3-14 GHz by introducing two parasitic pins to compensate the distortion in the high frequency bands.

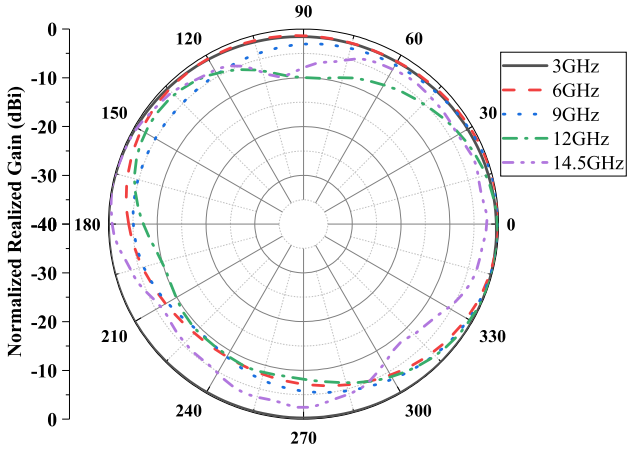

FIGURE 6. Normalized realized gain in the azimuth plane (XOY) of the proposed UWB antenna.

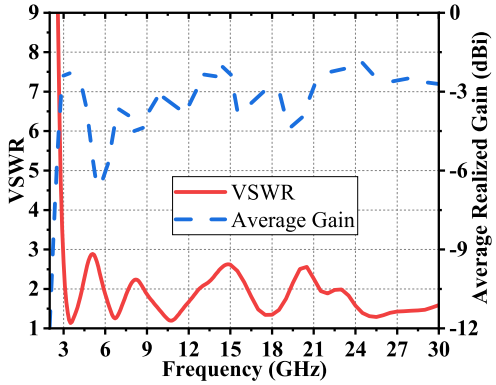

FIGURE 7. Simulated VSWR and average realized gain in the azimuth plane of the proposed UWB antenna.

The normalized realized gain in the azimuth plane (XOY) of the proposed UWB antenna is shown in Fig. 6. The bandwidth of the proposed antenna with horizontal radiation omnidirectionality ripple better than ±5 dB is more than 3-14.5 GHz. The VSWR and average realized gain in the azimuth plane of the proposed antenna are presented in Fig. 7. The impedance bandwidth is greater than 10:1 (2.96-30 GHz) for VSWR $<$ 3. The realized average gain in the azimuth plane is around −3 dBi for 3-10 GHz (UWB application).

C. PERFORMANCE OF UWB ANTENNA

The prototype and fabrication of the proposed UWB antenna are shown in Fig. 1 and Fig. 8, respectively. The proposed antenna is fabricated using 3D printing, as presented in Fig. 8 (a). The measurements are implemented by the Agilent network analyzer (Agilent N5230A) and far-field measurement system (NSI 2000) in the anechoic chamber, as shown in Fig. 8(b).

The simulated and measured VSWRs and realized peak gains in the azimuth plane (XOY) of the proposed antenna are displayed in Fig. 9. The impedance bandwidth of the proposed antenna is over 3-15 GHz. The realized peak gain in the azimuth plane is from −4 to 2.5 dBi. The simulated and

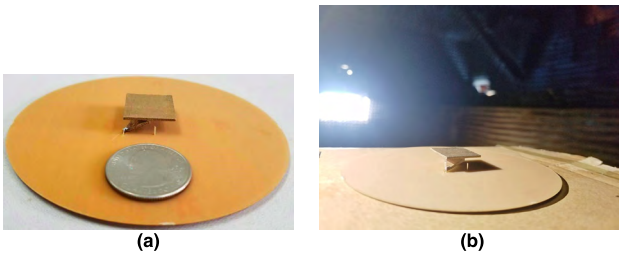

FIGURE 8. The fabrication of the proposed UWB antenna. (a) Photograph. (b) Measurement in the anechoic chamber.

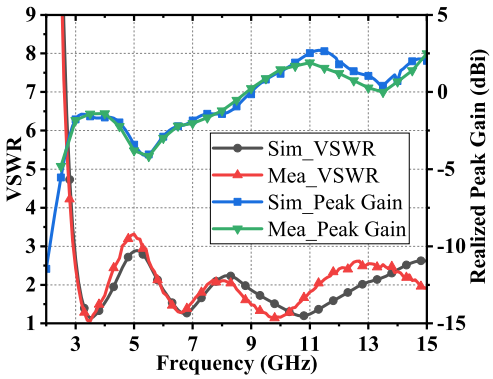

FIGURE 9. Simulated and measured VSWRs and realized peak gains in the azimuth plane of the proposed antenna.

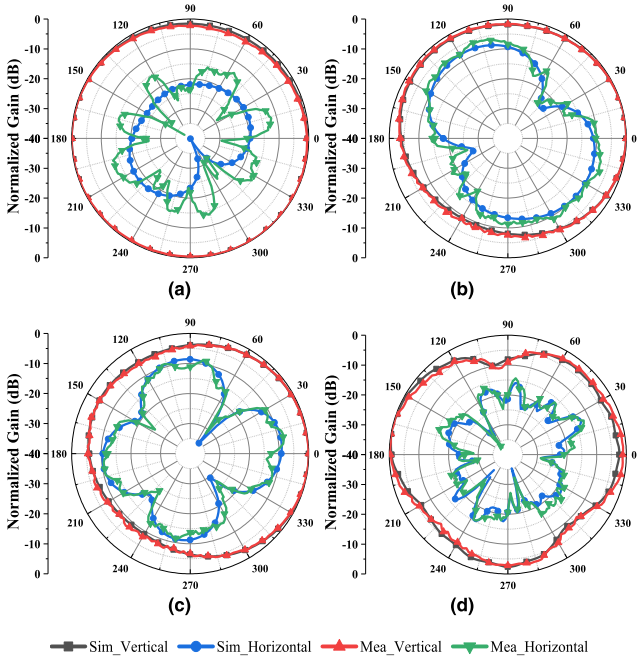

FIGURE 10. Vertically and horizontally polarized normalized gains in the azimuth plane at (a) 3 GHz, (b) 6 GHz, (c) 9 GHz, and (d) 14.5 GHz.

measured normalized gains with vertically and horizontally polarization in the azimuth plane at 3 GHz, 6 GHz, 9 GHz and 14.5 GHz are shown in Fig. 10. The bandwidth of the proposed UWB antenna with omnidirectionality better than ±5 dB is over 3-14.5 GHz. The measured results agree well with the simulated ones. The deviation between the simulated

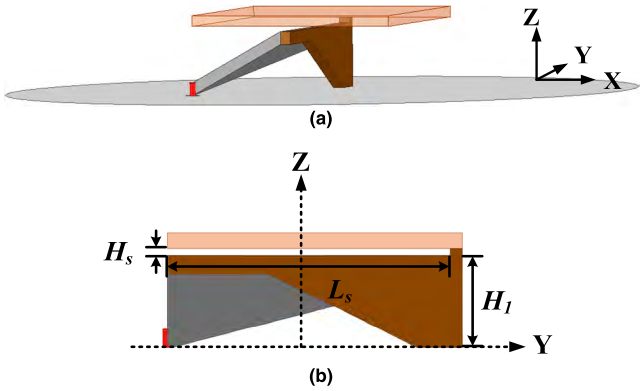

FIGURE 11. The proposed band-notched antenna. (a) Perspective view. (b) Side view. (L_s = 18.5 mm, H_s = 0.5 mm, H_1 = 6 mm).

results and measured ones is mainly because of the fabrication tolerance.

III. ANALYSIS OF BAND-NOTCHED ANTENNA

A. STRUCTURE OF BAND-NOTCHED ANTENNA

In order to introduce a deep notched band, the UWB antenna is modified by adding a split gap inside the antenna without changing other parameter values. As the proposed band-notched antenna is shown in Fig.11, the split gap with the length L_s of 18.5 mm and the height H_s of 0.5 mm is placed between the capacitive top hat and the feeding and shorted structures.

B. ANALYSIS OF BAND-NOTCHED ANTENNA

The simulated VSWRs, radiation efficiencies and realized peak gains in the azimuth plane (XOY) of the UWB and the band-notched antennas are displayed in Fig. 12(a), (b) and (c), respectively. It can be seen from Fig. 12(a) that a deep notched band can be achieved at 3.5 GHz with the impedance bandwidth of 2.4-2.5 and 5-12 GHz for VSWR < 2. As depicted in Fig. 12(b), the radiation efficiency of the notched band is suppressed and the efficiency for 2.4/5 GHz WLAN bands are better than 89%. Fig. 12(c) shows that the horizontal realized peak gain at 3.5 GHz is suppressed from -1.6 dBi to -25 dBi, and the gain for 2.4-2.5 GHz can be improved to 0 dBi.

Two important parameters, the length L_s and the height H_s of the split gap, are analyzed to study the impacts on VSWR of the proposed band-notched antenna, as presented in Fig. 13(a) and (b), respectively. Fig. 12(a) shows that by increasing the length L_s, the notched band and the lowest operating frequency can be moved towards the lower frequency. So, large L_s value is chosen to miniaturize the antenna and have the notched band resonant at 3.5 GHz. Fig. 12(b) displays that when the height H_s increases from 0.2 mm to 0.8 mm, the bandwidth of the notched band would become larger, and the lowest operating frequency moves downwards the lower frequency. Therefore, suitable H_s value is adopted

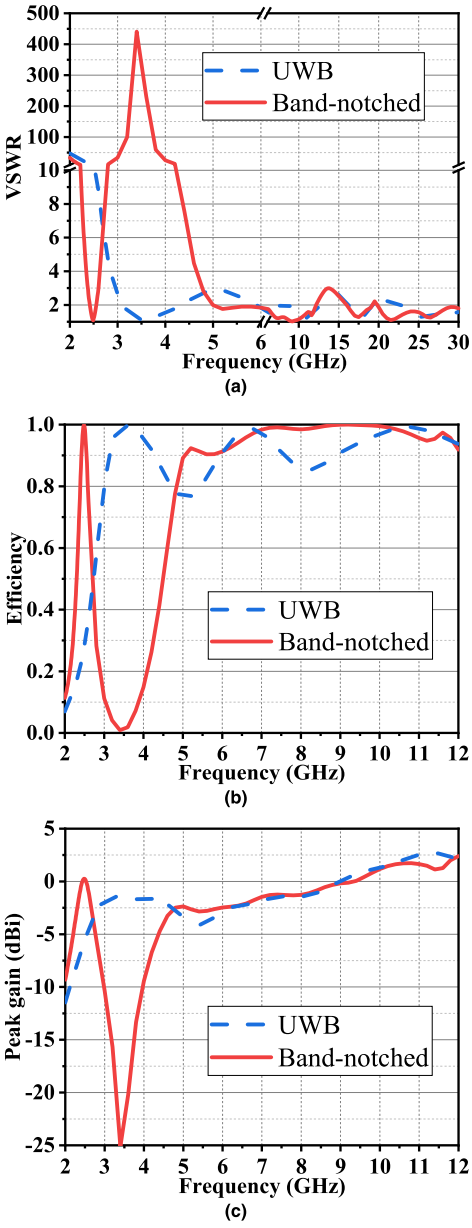

FIGURE 12. Simulated (a) VSWRs, (b) radiation efficiencies and (c) realized peak gains of the proposed UWB and band-notched antennas.

to determine the bandwidth of the notched band and achieve two operating bands for the 2.4/5 GHz WLAN applications.

C. PERFORMANCE OF BAND-NOTCHED ANTENNA

The prototype and fabrication of the proposed band-notched antenna are shown in Fig. 11 and Fig. 14, respectively. The proposed band-notched antenna is also fabricated using 3D printing and installed on a metallic ground.

The simulated and measured VSWRs and realized peak gains in the azimuth plane (XOY) are plotted in Fig. 15(a) and (b), respectively. The measured notched band is centered at 3.4 GHz, as displayed in Fig. 15(a). The measured impedance bandwidth of the proposed antenna is 2.4-2.5 GHz and 5-10 GHz for VSWR < 2. Fig. 15(b) shows

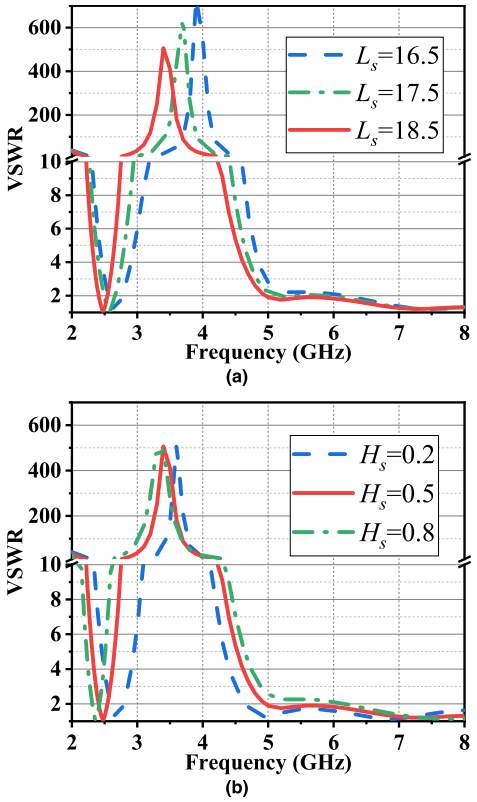

FIGURE 13. Impacts of (a) L_S and (b) H_S on VSWR of the proposed band-notched antenna.

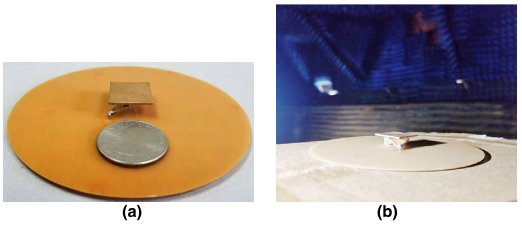

FIGURE 14. The fabrication of the proposed band-notched antenna. (a) Photograph view. (b) Measurement in the anechoic chamber.

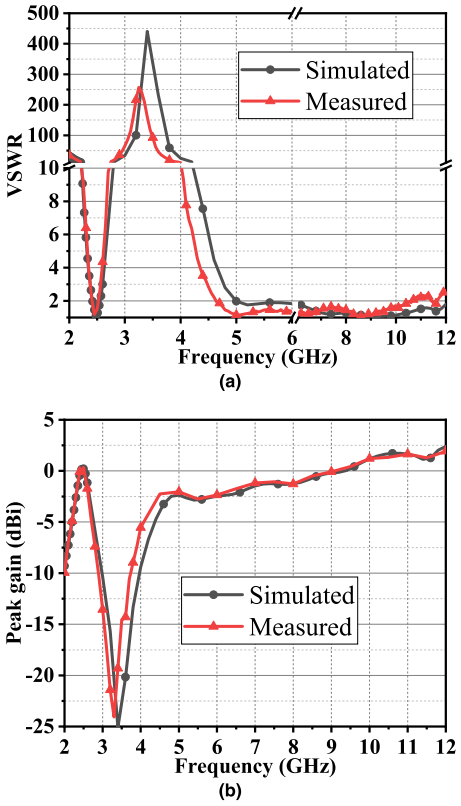

FIGURE 15. Simulated and measured (a) VSWRs and (b) realized peak gains in the azimuth plane of the proposed band-notched antenna.

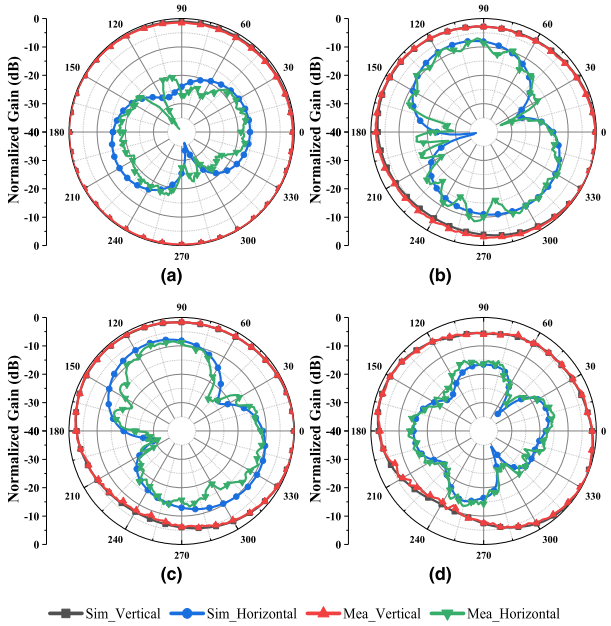

FIGURE 16. Vertically and horizontally polarized normalized gains in the azimuth plane at (a) 2.4 GHz, (b) 5.2 GHz, (c) 5.8 GHz, and (d) 10 GHz.

that the realized peak gain at 3.5 GHz is suppressed from −1.6 dBi to −25 dBi, and the gain for 2.4-2.5 GHz can be improved to 0 dBi. The measured results meet well with the simulated ones. The deviation between the simulated and measured results is mainly due to the fabrication tolerance.

The simulated and measured normalized gains with vertically and horizontally polarization in the azimuth plane (XOY) at 2.4 GHz, 5 GHz, 6 GHz and 10 GHz are depicted in Fig. 16. The horizontal radiation pattern omni-directionality ripple of the proposed band-notched antenna is better than ±5 dB for 2.4-2.5 GHz and 5-10 GHz, which can be used in the WLAN applications.

Table I displays the comparison among the two proposed antennas and other UWB antennas. All the reference antennas have UWB bandwidth with monopole-like radiation patterns. As discussed in the Introduction, works in [7], [8] using capacitive ceiling-mount loading have relatively large volume. Antennas in [9]–[15] utilize capacitive top hat with four shorted posts to realize compact size and low profile. The work [15] miniaturizes the omnidirectional antenna using dielectric material and meander shorted lines with $k_{\min}a = 0.68$. Works [16]–[19] use capacitive top hat

TABLE 1. Comparison of Different Antennas.

Ref.	Structure Type	Element Size/λ_L	BW	k_La	Radiation Efficiency	Matching Circuit
[7]	Cylinder	D=0.4; H=0.221	6.92:1	1.87	n/a	No
[8]	Cylinder	D=0.32; H=0.184	9.23:1	1.53	>78%	No
[9]	Cylinder	D=0.36; H=0.068	3:1	1.21	n/a	No
[10]	Cube	W=0.204; H=0.087	3.9:1	1.06	>95%	No
[11]	Cylinder	D=0.36; H=0.053	6.67:1	1.18	n/a	No
[12]	Cylinder	D=0.144; H=0.143	6.5:1	1.01	n/a	No
[13]	Cube	W=0.208; H=0.068	2.91:1	1.02	>97%	No
[14]	Cube	W=0.3; H=0.075	6.64:1	1.41	n/a	No
[15]	Cylinder	D=0.115; H=0.092	4.86:1	0.68	>80%	No
[16]	Cylinder	D=0.19; H=0.085	5.5:1	0.803	>60%	Yes
[17]	Cube	W=0.22; H=0.033	4:1	1.00	>80%	Yes
[18]	Cube	W=0.26; H=0.046	8.5:1	1.19	>70%	Yes
[19]	Cylinder	D=0.144; H=0.09	4.1:1	0.73	>95%	No
Proposed UWB	**Cube**	**W=0.19; H=0.06**	**10:1**	**0.92**	**>76%**	**No**
Band-notched	**Cube**	**W=0.152; H=0.052**	**WLAN**	**0.75**	**>89%**	**No**

D and H are the diameter and the height of the antennas with cylindrical structures. W and H are the width and the height of the antenna with rectangular structures. k_L is the wavenumber at the lowest operating frequency of the antenna.

with only two shorted posts to realize compact volume, and the work [18] utilizes two antennas and an extra duplexer to compensate the radiation pattern distortion in the higher band. The proposed UWB antenna can achieve electrically small size and UWB characteristic with good omnidirectionality without extra matching circuit. Two parasitic pins are utilized to improve the radiation pattern ripple performance in the azimuth plane. Moreover, the UWB antenna can be modified to realize dual-band characteristic with a deep band-notch for 2.4/5 GHz WLAN applications.

IV. CONCLUSION

Firstly, a 3D printed, compact, low-profile, UWB antenna with monopole-like radiation characteristics is proposed in this paper. The proposed UWB antenna can realize small volume of $0.19\lambda_L \times 0.19\lambda_L \times 0.06\lambda_L$. The impedance bandwidth is over 10:1 (2.96-30 GHz) for VSWR < 3, and the horizontal radiation pattern ripple is better than ± 5 dB for 2.96-14.5 GHz. Secondly, this UWB design is also modified to realize dual bands with a deep band-notch by adding a split gap inside the antenna. The proposed band-notched antenna is designed with the bandwidth of 2.4-2.5 and 5-10 GHz for VSWR < 2 with good omnidirectional performance, which can be used for 2.4/5 GHz WLAN applications.

REFERENCES

[1] A. Alipour and H. R. Hassani, "A novel omni-directional UWB monopole antenna," *IEEE Trans. Antennas Propag.*, vol. 56, no. 12, pp. 3854–3857, Dec. 2008.

[2] H. Zhai, S. Tjuatja, J. W. Bredow, and M. Lu, "A quasi-planar conical antenna with broad bandwidth and omnidirectional pattern for ultrawideband radar sensor network applications," *IEEE Trans. Antennas Propag.*, vol. 58, no. 11, pp. 3480–3489, Nov. 2010.

[3] W. S. Yeoh and W. S. T. Rowe, "An UWB conical monopole antenna for multiservice wireless applications," *IEEE Antennas Wireless Propag. Lett.*, vol. 14, no. , pp. 1085–1088, 2015.

[4] R. Lian, T. Shih, Y. Yin, and N. Behdad, "A high-isolation, ultra-wideband simultaneous transmit and receive antenna with monopole-like radiation characteristics," *IEEE Trans. Antennas Propag.*, vol. 66, no. 2, pp. 1002–1007, Feb. 2018.

[5] L. Zhao, Z.-M. Chen, and J. Wang, "A wideband dual-polarized omnidirectional antenna for 5G/WLAN," *IEEE Access*, vol. 7, pp. 14266–14272, 2019.

[6] J. Zhao, D. Psychoudakis, C.-C. Chen, and J. L. Volakis, "Design optimization of a low-profile UWB body-of-revolution monopole antenna," *IEEE Trans. Antennas Propag.*, vol. 60, no. 12, pp. 5578–5586, Dec. 2012.

[7] L. Zhou, Y.-C. Jiao, Y. Qi, Z. Weng, and T. Ni, "Wideband ceiling mount omnidirectional antenna for indoor distributed antenna system applications," *Electron. Lett.*, vol. 50, no. 4, pp. 253–255, Feb. 2014.

[8] L. Zhou, Y. Jiao, Y. Qi, Z. Weng, and L. Lu, "Wideband ceiling-mount omnidirectional antenna for indoor distributed antenna systems," *IEEE Antennas Wireless Propag. Lett.*, vol. 13, pp. 836–839, 2014.

[9] D. W. Aten and R. L. Haupt, "A wideband, low profile, shorted top hat monocone antenna," *IEEE Trans. Antennas Propag.*, vol. 60, no. 10, pp. 4485–4491, Oct. 2012.

[10] M. Koohestani, J.-F. Zürcher, A. Moreira, and A. Skrivervik, "A novel, low-profile, vertically-polarized UWB antenna for WBAN," *IEEE Trans. Antennas Propag.*, vol. 62, no. 4, pp. 1888–1894, Apr. 2014.

[11] A. Elsherbini and K. Sarabandi, "Very low-profile top-loaded UWB coupled sectorial loops antenna," *IEEE Antennas Wireless Propag. Lett.*, vol. 10, pp. 800–803, 2011.

[12] H. Nakano, H. Iwaoka, K. Morishita, and J. Yamauchi, "A wideband low-profile antenna composed of a conducting body of revolution and a shorted parasitic ring," *IEEE Trans. Antennas Propag.*, vol. 56, no. 4, pp. 1187–1192, Apr. 2008.

[13] N. Nguyen-Trong, A. Piotrowski, T. Kaufmann, and C. Fumeaux, "Low-profile wideband monopolar UHF antennas for integration onto vehicles and helmets," *IEEE Trans. Antennas Propag.*, vol. 64, no. 6, pp. 2562–2568, Jun. 2016.

[14] H. Nakano, M. Takeuchi, and J. Yamauchi, "Low-profile wideband iCROSS antenna," *IEEE Trans. Antennas Propag.*, vol. 64, no. 7, pp. 2824–2831, Jul. 2016.

[15] A. A. Omar and Z. Shen, "A compact and wideband vertically polarized monopole antenna," *IEEE Trans. Antennas Propag.*, vol. 67, no. 1, pp. 626–631, Jan. 2019.

[16] S. M. A. M. H. Abadi and N. Behdad, "An electrically small, vertically polarized ultrawideband antenna with monopole-like radiation characteristics," *IEEE Antennas Wireless Propag. Lett.*, vol. 13, pp. 742–745, 2014.

[17] N. Behdad, M. Li, and Y. Yusuf, "A very low-profile, omnidirectional, ultrawideband antenna," *IEEE Antennas Wireless Propag. Lett.*, vol. 12, pp. 280–283, 2013.

[18] K. Ghaemi and N. Behdad, "A low-profile, vertically polarized ultrawideband antenna with monopole-like radiation characteristics," *IEEE Trans. Antennas Propag.*, vol. 63, no. 8, pp. 3699–3705, Aug. 2015.

[19] M. Li and N. Behdad, "A compact, capacitively fed UWB antenna with monopole-like radiation characteristics," *IEEE Trans. Antennas Propag.*, vol. 65, no. 3, pp. 1026–1037, Mar. 2017.

[20] Y. Y. Kyi and J.-Y. Li, "Analysis of electrically small size conical antennas," *Prog. Electromagn. Res. Lett.*, vol. 1, pp. 85–92, 2008.

[21] S. Palud, F. Colombel, M. Himdi, and C. Le Meins, "Wideband omnidirectional and compact antenna for VHF/UHF band," *IEEE Antennas Wireless Propag. Lett.*, vol. 10, pp. 3–6, 2011.

[22] H. Moon, G.-Y. Lee, C.-C. Chen, and J. L. Volakis, "An extremely low-profile ferrite-loaded wideband VHF antenna design," *IEEE Antennas Wireless Propag. Lett.*, vol. 11, pp. 322–325, 2012.

YAOHUI ZHANG received the B.S. degree in electromagnetic wave propagation and antenna from the University of Electronic Science and Technology of China (UESTC), Chengdu, China, in 2014, where he is currently pursuing the Ph.D. degree in electromagnetic field and microwave technology.

His research interests include compact and wideband antennas, and microwave filter.

YONGHONG ZHANG received the B.S., M.S., and Ph.D. degrees from the University of Electronic Science and Technology of China (UESTC), Chengdu, China, in 1992, 1995, and 2001, respectively.

He is currently a Full Professor with the School of Electronic Science and Engineering, UESTC, where he was a Lecturer, from 1995 to 2002. From 2002 to 2004, he was a Postdoctoral Fellow with the Department of Electronic Engineering, Tsinghua University, Beijing, China. Since 2004, he has been with UESTC. His research interests include microwave and millimeter-wave technology and applications. He is a Senior Member of the Chinese Institute of Electronics.

DAOTONG LI (S'15–M'16) received the Ph.D. degree in electromagnetic field and microwave technology from the University of Electronic Science and Technology of China (UESTC), Chengdu, China, in 2016.

He is currently with the Center of Aircraft TT&C and Communication, Chongqing University, Chongqing. Since 2015, he has been a Visiting Researcher with the Department of Electrical and Computer Engineering, University of Illinois at Urbana–Champaign, Urbana, IL, USA, with financial support from the China Scholarship Council. He has authored or coauthored over 50 peer-reviewed journals or conference papers. Since 2014, he has been a reviewer for some international journals. His current research interests include RF, microwave and millimeter-wave technology and applications, antennas, devices, circuits and systems, and passive and active (sub-) millimeter-wave imaging and radiometer.

Dr. Li was a recipient of the UESTC Outstanding Graduate Awards by the Sichuan Province and UESTC, in 2016. He was a recipient of the National Graduate Student Scholarship from the Ministry of Education, China, and ''Tang Lixin'' Scholarship. He is serving as a reviewer for several IEEE and IET journals, and as a TPC member, the Session Organizer, and the Session Chair for many international conferences.

ZHONGQIAN NIU was born in Luoyang, Henan, China, in 1991. He received the B.E. degree in electronic science and technology from the University of Electronic Science and Technology of China (UESTC), Chengdu, China, in 2014, where he is currently pursuing the Ph.D. degree in terahertz solid-state devices and systems with the School of Electronic Science and Engineering.

His research interests include terahertz high speed communication system, terahertz mixers, and other terahertz devices.

YONG FAN (M'05) received the B.E. degree from the Nanjing University of Science and Technology, Jiangsu, China, in 1985, and the M.S. degree from the University of Electronic Science and Technology of China (UESTC), Chengdu, China, in 1992.

He is currently a Full Professor with the School of Electronic Science and Engineering, University of Electronic Science and Technology of China. His current research interests include electromagnetic theory, millimeter-wave and terahertz circuits, communication technology, and so on. He has authored or coauthored more than 200 papers. He is a Senior Member of the Chinese Institute of Electronics.